Electrochemistry Communications 13 (2011) 886–889

Contents lists available at ScienceDirect

Electrochemistry Communications

journal homepage: www.elsevier.com/locate/elecom

Pt_1-Pd_3Co_1 nanoparticles supported on multi-walled carbon nanotubes as a high performance electrocatalyst for methanol oxidation

Yuming Guo, Chuangang Hu, Lin Yang *, Zhengyu Bai, Kui Wang, Shujun Chao

College of Chemistry and Environmental Science, Henan Normal University, Engineering Technology Research Center of Motive Power and Key Materials of Henan Province, Xinxiang 453007, PR China

ARTICLE INFO

Article history:
Received 12 April 2011
Received in revised form 23 May 2011
Accepted 26 May 2011
Available online 2 June 2011

Keywords:
Electrocatalysts
Noble metal
Heteronanostructures
Pristine-MWCNTs
Methanol oxidation

ABSTRACT

In this communication, a high performance heteronanostructured electrocatalyst for methanol oxidation, Pt decorating PdCo nanoparticles supported on pristine multi-walled carbon nanotubes (Pt_1-Pd_3Co_1/P-MWCNTs), is successfully prepared *via* a two-step strategy. Cyclic voltammetry and chronoamperometry measurements demonstrate that the as-prepared Pt_1-Pd_3Co_1/P-MWCNTs catalyst exhibits superior electrocatalytic performance for methanol oxidation compared with commercial 20% Pt/C and Pt/P-MWCNTs catalysts. Furthermore, the mass activity of the as-prepared Pt_1-Pd_3Co_1/P-MWCNTs catalyst is about 3 times of that of the Pt/P-MWCNTs catalyst. The enhanced electrocatalytic activity and stability could be attributed to the synergistic effect between Pt and PdCo, resulting in the higher utilization efficiency of Pt. Because of its relatively low-cost and high performance, the as-prepared Pt_1-Pd_3Co_1/P-MWCNTs catalyst might be an economically viable alternative for methanol oxidation.

1. Introduction

As a commercially viable alternative power source for small portable electronic devices, direct methanol fuel cells (DMFCs) have attracted considerable interest because of the easy fuel storage, simple structure, high energy efficiency, and low operating temperature [1]. Pt and Pt-based nanoparticles are of major interest as anode catalysts for DMFCs [2]. However, the high costs associated with high Pt loadings severely limit the corresponding applications. Therefore, on the one hand, the Pt-based alloys were studied extensively to improve the utilization efficiency of Pt to reduce its loading and the cost of the catalysts. However, the rigorous alloying conditions significantly hinder the application perspectives. Recently, Pt-based heteronanostructures have attracted tremendous attention [3,4]. On the other hand, the choice of the support is another key factor affecting the electrocatalytic performance of the catalysts [5]. Owing to the high electrical conductivity, large surface area, and chemical stability, multi-walled carbon nanotubes (MWCNTs) are considered as an attractive support for electrocatalysts [6]. However, the prerequisite functionalization of the MWCNTs, generally through oxidative treatments, inevitably impaired the mechanical properties, reduced the electrical conductivity and corrosion resistance, and thereby reduced the electrocatalytic activity of the catalysts [7]. Therefore, it is still a great challenge to anchor and deposit the catalyst nanoparticles onto the surface of the pristine MWCNTs (P-MWCNTs).

Herein, a ternary heteronanostructured electrocatalyst supported on P-MWCNTs, Pt_1-Pd_3Co_1/P-MWCNTs, is successfully prepared. The reasons for the selection of Pt, Pd, and Co are: (i) Pd and Co could form binary alloy with face-centered cubic (fcc) structure under certain conditions, which favors the reductive deposition of Pt [8]. (ii) Pd is good oxygen bond cleaving metal, favoring the enhancement of the electrooxidation activity for methanol [9]. (iii) The good thermoconductivity of Pd might inhibit the sintering and agglomeration of Pt, thereby enhance the corresponding electrochemical durability. (iv) Pd is widespread in the earth's crust, it's less expensive and stable in acidic electrolytes [10]. The electrochemical measurements indicate the Pt_1-Pd_3Co_1/P-MWCNTs exhibit enhanced electrocatalytic activity toward methanol oxidation, about 3 times of that of the Pt/P-MWCNTs. This reveals that the as-prepared Pt_1-Pd_3Co_1/P-MWCNTs might be a superior candidate for DMFCs applications.

2. Experimental

2.1. Catalyst preparation

Herein, a two-step strategy was used to prepare the Pt_1-Pd_3Co_1/P-MWCNTs catalyst (Scheme 1). Firstly, $PdCl_2$, $CoCl_2$, and glutamate were added into glycerin and the pH was adjusted to 13. Subsequently, P-MWCNTs were added, and the mixture was ultrasonicated and stirred to obtain a homogeneous suspension. Then, the suspension was heated at 180 °C for 6 h in a Teflon-lined autoclave. The product was filtered, dried, and denoted as Pd_3Co_1/P-MWCNTs. Secondly, the Pd_3Co_1/P-MWCNTs were ultrasonically suspended into a mixed solution of ethylene glycol and double distilled water.

* Corresponding author. Tel.: +86 373 3325999; fax: +86 373 3328507.
E-mail address: yanglin1819@163.com (L. Yang).

1388-2481/$ – see front matter © 2011 Elsevier B.V. All rights reserved.
doi:10.1016/j.elecom.2011.05.030

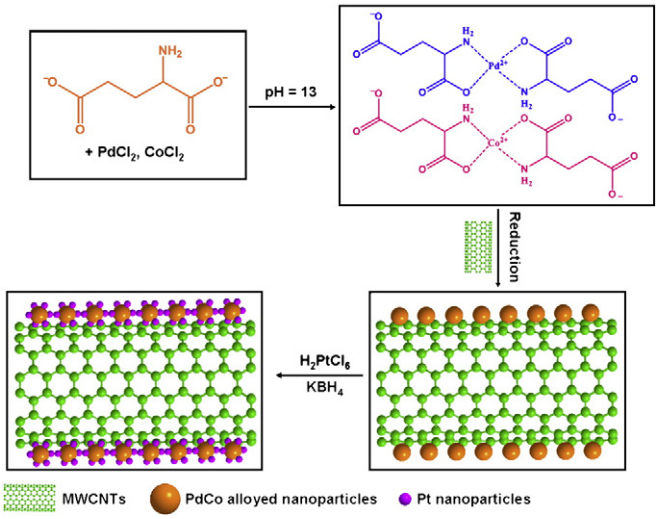

Scheme 1. Formation mechanism of the Pt_1-Pd_3Co_1/P-MWCNTs catalyst.

The resulted ink was mixed with H_2PtCl_6 and stirred for 2 h. Then a freshly prepared KBH_4 solution was added and stirred for another 2 h. Subsequently, the suspension was filtered and dried under vacuum. Finally, the Pt_1-Pd_3Co_1/P-MWCNTs catalyst was obtained.

In addition, control experiment was performed under the same conditions as the second step of the typical experiment. The obtained Pt catalyst supported on P-MWCNTs was denoted as Pt/P-MWCNTs.

2.2. Catalyst characterization

The composition of the Pt_1-Pd_3Co_1/MWCNTs was evaluated by inductively coupled plasma-mass spectrometry (ICP-MS) analysis. The particle sizes, morphologies, and energy dispersive spectra (EDS) of the catalysts were determined by high resolution transmission electron microscopy (HR-TEM). The X-ray diffraction (XRD) patterns of the catalysts were recorded with a Cu Kα radiation source.

2.3. Electrochemical measurements

The electrochemical measurements were performed in a three-electrode cell system. A glassy carbon disk (0.0706 cm^2) coated with catalyst, an Ag/AgCl electrode, and a platinum foil (1 cm^2) were used as the working, reference, and counter electrodes, respectively. All potentials are recalculated with respect to the standard hydrogen electrode (SHE). Briefly, the working electrode was prepared as follows: 5 mg of catalyst was added into 0.5 mL of ethanol and 50 μL of 5 wt.% perfluorosulfonic acid solution and ultrasonicated to obtain a homogeneous ink. Next, the ink was uniformly dispersed onto a glassy carbon electrode.

3. Results and discussion

From the ICP-MS analysis, the atomic ratio of Pt, Pd and Co in the Pt_1-Pd_3Co_1/P-MWCNTs is ca. 1:3:1. The practical percentage of the Co in the catalyst is only half of the theoretical percentage, indicating the surface displacement reaction occurred between Co and H_2PtCl_6.

Fig. 1A–B shows the TEM images of the Pd_3Co_1/P-MWCNTs and Pt_1-Pd_3Co_1/P-MWCNTs catalysts, respectively. From Fig. 1A, Pd_3Co_1 alloyed nanoparticles with the average size of 7.2 nm evenly deposited on the surface of the P-MWCNTs. This might be attributed to the cross-linking effect of the glutamate [11]. From Fig. 1B, small Pt nanoparticles with the average size of 1.8 nm are decorated on the Pd_3Co_1 nanoparticles uniformly. This might be attributed to the same fcc structures of Pt and Pd_3Co_1 nanoparticles, which favor the growth

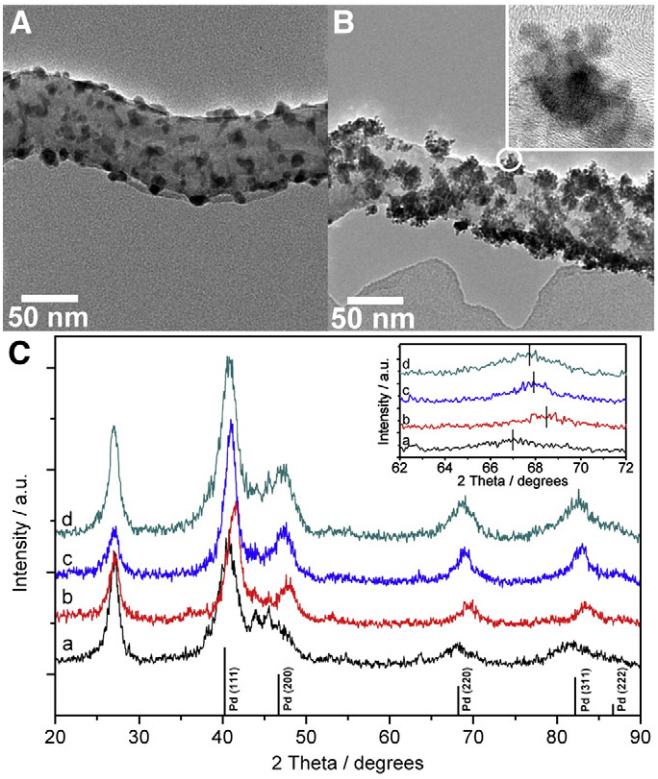

Fig. 1. The TEM images of (A) Pd_3Co_1/P-MWCNTs and (B) Pt_1-Pd_3Co_1/P-MWCNTs catalysts, inset: the region of white circle at high magnification, and (C) XRD patterns of (a) Pd/P-MWCNTs (b) Pd_3Co_1/P-MWCNTs, (c) Pt_1-Pd_3Co_1/P-MWCNTs, and (d) Pt/P-MWCNTs catalysts.

of Pt on the surface of the alloyed nanoparticles [8]. The small particle size would be beneficial to the enhancement of the electrocatalytic performance.

Fig. 1C presents the XRD patterns of different catalysts. From the figure, the first peak at 26.0° is assigned to the graphite (002) plane of the P-MWCNTs, and the other four peaks at 39.7, 46.4, 67.7, and 81.9° are assigned to planes (111), (200), (220), and (311) of fcc Pt (Pd, Pd_3Co_1 alloy), respectively. Compared with the Pd/P-MWCNTs, the lattice spaces of the Pd_3Co_1/P-MWCNTs show the slightly positive shift, indicating a lattice contraction. Furthermore, no peaks related to Co are observed. These indicate the Co enter into the Pd lattice to form the PdCo alloy [12]. Moreover, the composition of the Pt_1-Pd_3Co_1/P-MWCNTs was determined as Pt, Pd, Co, and C by EDS analysis. In addition, the XRD pattern of the Pt_1-Pd_3Co_1/P-MWCNTs is almost same as the Pt/P-MWCNTs, the diffraction peaks of the bare Pd_3Co_1 alloy are hardly observed. This can be attributed to the decorating effect of the Pt nanoparticles on the alloyed nanoparticles.

The electrochemical behaviors of different catalysts were determined by cyclic voltammetry (CV) in 0.5 M H_2SO_4 and the results are shown in Fig. 2A. From the figure, the current densities in the hydrogen adsorption/desorption and oxide formation/reduction of the Pt_1-Pd_3Co_1/P-MWCNTs are much larger than those of the Pt/P-MWCNTs and JM 20% Pt/C. The area of hydrogen adsorption peak for Pt_1-Pd_3Co_1/MWCNTs is much larger than those of the Pt/MWCNTs, and JM 20% Pt/C catalysts, which is most likely due to the hydrogen absorption of the bulk Pd. Interestingly, there were also suggestions that metal dissolution was suppressed for Pd deposited in the presence of absorbing hydrogen [13].

The electrocatalytic activities of different catalysts for methanol oxidation were determined by CV in 0.5 M H_2SO_4 and 0.5 M CH_3OH and the results are shown in Fig. 2B. Based on the Pt percentages in Pt_1-Pd_3Co_1/P-MWCNTs (11.2%) and Pt/P-MWCNT (13.1%)

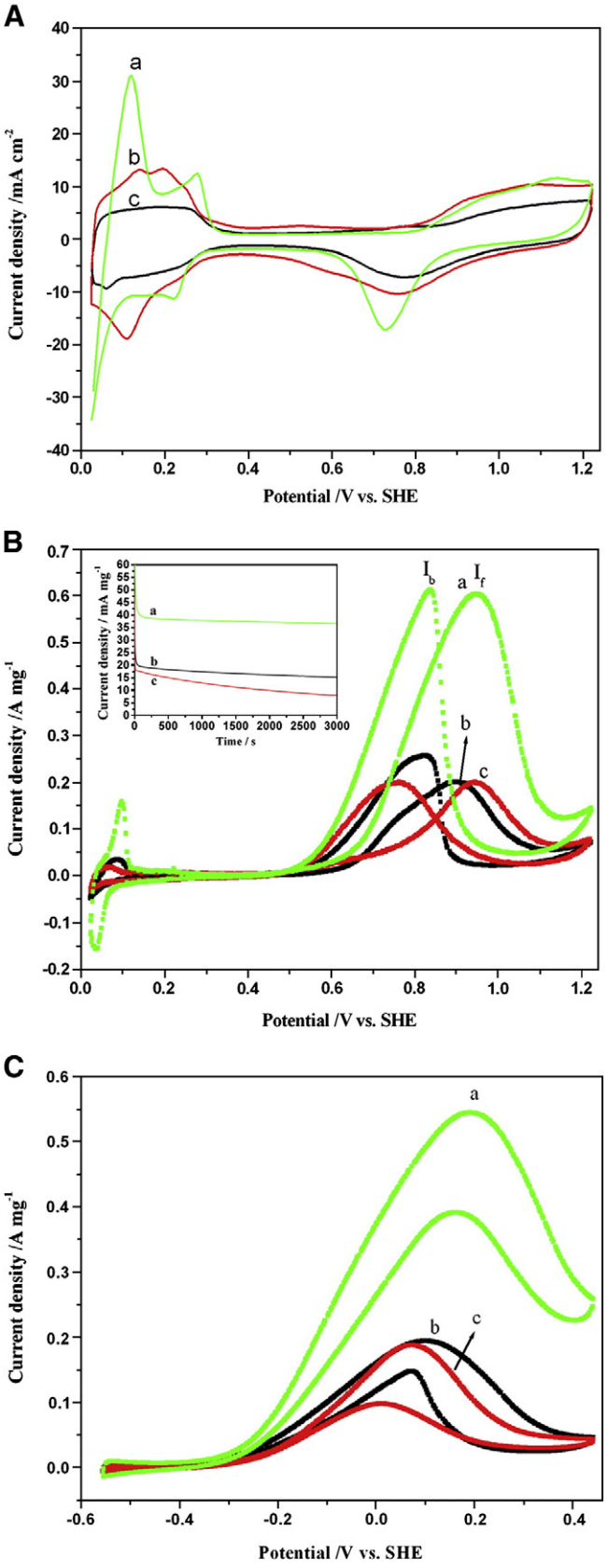

Fig. 2. (A) CV of (a) Pt_1-Pd_3Co_1/P-MWCNTs, (b) JM 20% Pt/C, and (c) Pt/P-MWCNTs catalysts in 0.5 M H_2SO_4 solution with the scan rate of 20 mV s^{-1} at 20 ± 1 °C. (B) CV of (a) Pt_1-Pd_3Co_1/P-MWCNTs, (b) JM 20% Pt/C, and (c) Pt/P-MWCNTs catalysts in 0.5 M H_2SO_4 + 0.5 M CH_3OH solution. Inset shows the corresponding chronoamperometric curves. (C) CV of (a) Pt_1-Pd_3Co_1/P-MWCNTs, (b) JM 20% Pt/C, and (c) Pt/P-MWCNTs catalysts in 0.5 M KOH + 1 M CH_3OH solution.

determined by ICP-MS, the mass activity defined as the current related to the amount of deposited platinum of the Pt_1-Pd_3Co_1/P-MWCNTs is 0.608 A mg^{-1}, about 3 times of those of the JM 20% Pt/C (0.206 A mg^{-1}) and Pt/P-MWCNT (0.207 A mg^{-1}). This indicates the heteronanostructure of the Pt_1-Pd_3Co_1/P-MWCNTs, especially the electronic effect between the Pt and the PdCo alloyed nanoparticles and the suitable "unimpaired" MWCNTs support, can effectively enhance the utilization efficiency of Pt and reduce the loading of Pt significantly. Consequently, the cost of the catalyst can be reduced significantly. In addition, the electrocatalytic activities of different catalysts for methanol oxidation in alkaline solution are shown in Fig. 2C. The current density of the Pt_1-Pd_3Co_1/P-MWCNTs in alkaline media is higher than those of the Pt/P-MWCNTs and JM 20% Pt/C, but is not as high as the hypothesis and is not equal to the sum of the Pt and Pd. This might be attributed to the covering effect of the Pt nanoparticles on the surface of the alloyed nanoparticles.

Additionally, two different anodic peaks were observed in the forward and reverse scans during the methanol oxidation. Generally, the ratio of the forward anodic peak current (I_f) to the reverse anodic peak current (I_b), I_f/I_b, could be used to describe the catalyst tolerance to the carbonaceous species on the electrode surface [14]. A higher ratio means the higher removal efficiency of the poisoning species. From Fig. 2B, the I_f/I_b ratio of the Pt_1-Pd_3Co_1/P-MWCNTs (0.98) is higher than that of the JM 20% Pt/C (0.80), showing the better tolerance to the intermediate carbonaceous species.

The long-term stability of the electrocatalysts is very important to the commercially viable DMFCs. The electrochemical stabilities of different catalysts for methanol oxidation were determined by chronoamperometry in 0.5 M H_2SO_4 and 0.5 M CH_3OH solution for 3000 s and the results are shown in the inset of Fig. 2B. Compared with the JM 20% Pt/C and Pt/P-MWCNTs catalysts, the Pt_1-Pd_3Co_1/P-MWCNTs exhibits the much higher anodic current and the slower current decay, indicating the better catalytic activity and stability for methanol oxidation. The enhanced stability of the Pt_1-Pd_3Co_1/P-MWCNTs was confirmed by TEM measurements after 500 CV cycles in 0.5 M H_2SO_4 and 0.5 M CH_3OH (Fig. 3). From the figure, serious sintering and agglomeration are observed for Pt/P-MWCNTs after 500 cycles. However, the morphology and dispersivity of the Pt_1-

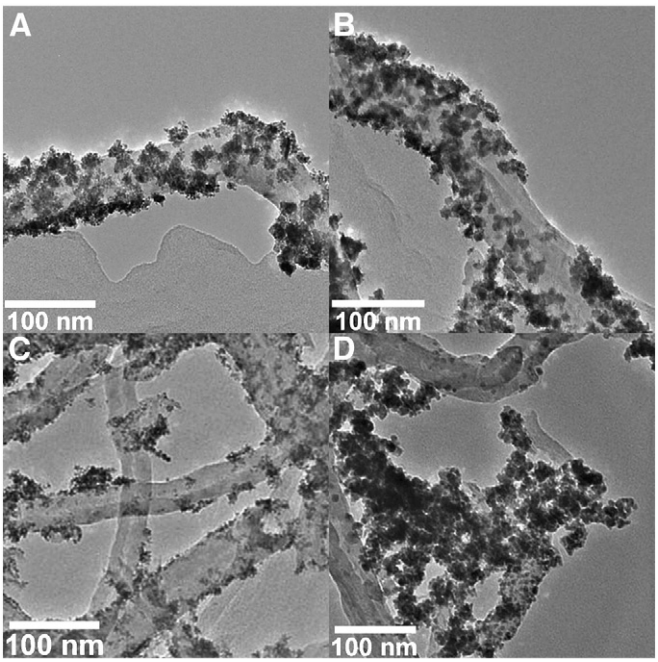

Fig. 3. TEM images of (A, B) Pt_1-Pd_3Co_1/MWCNTs and (C, D) Pt/MWCNTs before and after 500 potential cycles.

Pd_3Co_1/MWCNTs are preserved after the test, indicating the enhanced electrocatalytic stability. This might be attributed to the strong attachment of Pt on PdCo alloys, the good thermoconductivity of the Pd_3Co_1 alloys, and the high corrosion resistance of the MWCNTs.

4. Conclusions

In summary, a low-Pt heteronanostructured electrocatalyst Pt_1-Pd_3Co_1/P-MWCNTs for methanol oxidation was successfully prepared by a two-step strategy. The electrochemical results demonstrate that the electrocatalytic activity and stability of the Pt_1-Pd_3Co_1/P-MWCNTs for methanol oxidation are significantly enhanced. The mass activity of the Pt_1-Pd_3Co_1/P-MWCNTs for methanol oxidation is about 3 times of that of the Pt/P-MWCNTs catalyst and the cost of the catalyst can be reduced significantly. Therefore, the as-prepared Pt_1-Pd_3Co_1/P-MWCNTs might be a superior candidate for DMFCs applications.

Acknowledgments

This work was financially supported by the National Key Basic Research and Development Program of China (Grant No. 2009CB626610) and Henan Key Proposed Program for Basic and Frontier Research (Grant No. 092300410120).

References

[1] B. Yang, A. Manthiram, Electrochem. Comm. 6 (2004) 231.
[2] C. Bock, C. Paquet, M. Couillard, G.A. Botton, B.R. MacDougall, J. Am. Chem. Soc. 126 (2004) 8028.
[3] B. Lim, M. Jiang, P.H.C. Camargo, E.C. Cho, J. Tao, X. Lu, Y. Zhu, Y. Xia, Science 324 (2009) 1302.
[4] V. Mazumder, M. Chi, K.L. More, S. Sun, J. Am. Chem. Soc. 132 (2010) 7848.
[5] Z. Bai, L. Yang, Y. Guo, Z. Zheng, C. Hu, P. Xu, Chem. Commun. 47 (2011) 1752.
[6] B. Xu, J. Guo, H. Jia, X. Yang, X. Liu, Catal. Today 125 (2007) 169.
[7] B. Wu, D. Hu, Y. Kuang, B. Liu, X. Zhang, J. Chen, Angew. Chem. Int. Edit. 48 (2009) 4751.
[8] R. Wang, H. Li, S. Ji, H. Wang, Z. Lei, Electrochim. Acta 55 (2010) 1519.
[9] R. Wang, H. Li, H. Feng, H. Wang, Z. Lei, J. Power Sources 195 (2010) 1099.
[10] W. Wang, R. Wang, S. Ji, H. Feng, H. Wang, Z. Lei, J. Power Sources 195 (2010) 3498.
[11] C. Hu, Z. Bai, L. Yang, J. Lv, K. Wang, Y. Guo, Y. Cao, J. Zhou, Electrochim. Acta 55 (2010) 6036.
[12] X. Wang, Y. Tang, Y. Gao, T. Lu, J. Power Sources 175 (2008) 784.
[13] M. Łukaszewski, T. Kędra, A. Czerwiński, Electrochem. Comm. 11 (2009) 978.
[14] T. Maiyalagan, F.N. Khan, Catal. Commun. 10 (2009) 433.